29th EPS Conference on Plasma Phys. and Contr. Fusion Montreux, 17-21 June 2002 ECA Vol. **26B**, P-1.096 (2002)

Transport reduction by rotation shear in tokamak edge turbulence

C.F.Figarella, S.Benkadda, P.Beyer, I. Voitsekhovitch
Equipe Dynamique des Systèmes Complexes, LPIIM,
CNRS–Université de Provence, Marseille, France

X. Garbet
Association Euratom–CEA sur la Fusion, CEA Cadarache, France
(Dated: June 13, 2002)

Effects of imposed $E \times B$ flow shear on transport driven by the edge turbulence are studied in the 3D global simulations of resistive pressure gradient driven turbulence. Transport reduction is found to be due to both a decrease of fluctuations amplitudes as in their relative phase. A scaling of the turbulent diffusivity and the fluctuation level with the $E \times B$ flow shear is deduced from these simulations. Turbulent diffusivity reduced at modest shear and continues to decrease as the shear increase till full stabilization. A striking similarity in the $E \times B$ shear dependent diffusivity between our simulations and experimental observations is found.

I. INTRODUCTION

Turbulent transport in edge tokamak plasmas can be greatly reduced in the presence of stable shear flow, creating an edge transport barrier. These barriers, a key signature of L–H transition (i.e., a transition from a low confinement state to a higher confinement state) arise spontaneously or after applying an external radial electric field[18]. In the latter case, the external biaising technique produces an edge transport barrier by driving the $E \times B$ flow shear. The $E \times B$ velocity shear in plasmas affects turbulence levels and transport both linearly[12] and nonlinearly[11], acting on the fluctuations amplitude as well as the relative phase between pressure and potential fluctuations[6]. Also, the scaling of turbulent transport coefficients with plasma parameters has been predicted[2–4]. Here, we consider a model problem and continue numerically the study of the $E \times B$ rotation shear effect on the resistive–pressure–gradient–driven turbulence and analyze its behavior in the presence of an imposed $E \times B$ flow shear. Such study is motivated by experiments with a biasing of the plasma edge where the effect of an externally generated $E \times B$ flow on the turbulence and transport has been investigated recently [8, 16]. Our simulations have been performed in the full toroidal geometry using the 3D resistive ballooning mode code [7]. In addition to the trivial results illustrating the $E \times B$ flow shear stabilization of the turbulent fluctuations and the reduction of the associated transport accompanied with the formation of the barrier on the pressure profile, we present here the analysis of the $E \times B$ shear effect on the fluctuation amplitude and the cross correlation between the pressure and electrostatic potential fluctuations. Other issues addressed in this study are the scaling of turbulent transport with the toroidal magnetic field, and the scaling of the fluctuation level with rotation shear. Finally, our numerical results are compared with analytical models as well as recent experiments where the edge biasing has been applied.

II. MODEL FOR RESISTIVE BALLOONING MODES

The normalized form of the resistive ballooning equations is [7] :

$$\frac{d}{dt}\Delta_\perp \phi = -\Delta_\parallel \phi - Gp + \nu \Delta_\perp^2 \phi, \tag{1}$$

$$\frac{dp}{dt} = \chi_\parallel \Delta_\parallel p + \chi_\perp \Delta_\perp p + S_0, \tag{2}$$

where $d/dt = \partial/\partial t + \{\phi, \cdot\}$, $\{f, g\} = \partial_x f \partial_y g - \partial_y f \partial_x g$. The last term in the right hand side of Eq.1 is added to generate the imposed $E \times B$ rotation shear,i.e., if the backreaction of the fluctuations is artificially suppressed, the component $m = n = 0$ of the ϕ_{mn} is collisionally damped to ϕ_0, the parameter ϵ stands for the strength of the imposed velocity shear ($0 \leq \epsilon < 1$). The simulations are performed for the magnetic configuration with a monotonic q–profile for the plasma layer located between the $q = 2$ and $q = 3$ rational surfaces. A standard ballooning transformation is used and

the modes with the toroidal number up to $n = 24$ are included in the simulations. A more detailed description of the code assumptions is given in Ref. [1].
The stabilizing effect of the $E \times B$ rotation shear on the RBM is studied by varying an externally imposed $E \times B$ flow with following definition: $\epsilon\partial_x^2\phi_0 = -\tau\partial_r E_r/B_0 = \epsilon/\cosh^2(\sigma x)$ (here E_r is the radial electric field, $\sigma^{-1} = 13.44$ the width of the shear layer). By this term and in a stationary state, the poloidal velocity $\partial_x\phi_{00}$ is colisionally damped to the imposed rotation $\epsilon\partial_x\phi_0$ with a characteristic time scale of the order of ν_{fric}^{-1} which has to be chosen small compared to our normalized time unit (and also to the viscous time scale $(\nu\sigma^2)^{-1} = 90$). Here we choose $\nu_{fric}^{-1} = 0.05$. The shear rate is defined as : $\omega_{E\times B} = \partial_r(E_r/B_0)$. Note that the total shear flow is the sum of the imposed plus the self generated one during these simulations

III. E × B SHEAR STABILIZATION OF THE TURBULENT FLUCTUATIONS AND TRANSPORT

The effect of the $E \times B$ flow shear on the resistive ballooning modes is studied by varying the value of ϵ, from 0 (shearless case) to 0.9 (strong shear case). First, we analyze its effect on the structure and properties of the RBM. Then the $E \times B$ shear scaling of the transport and fluctuation level is presented.
The effect of the $E \times B$ rotation shear on the radial structure of the RBM is illustrated in Fig. 1 (Left) where the contour plots of the electrostatic potential $\delta\phi$, pressure fluctuations δp, and turbulent flux, $\Gamma = \delta p\ \delta v_r$, (here, $\delta v_r = -\partial_y\delta\phi$) for the shearless case and for the case with intermediate ($\epsilon = 0.3$) and large shear ($\epsilon = 0.9$) are presented.

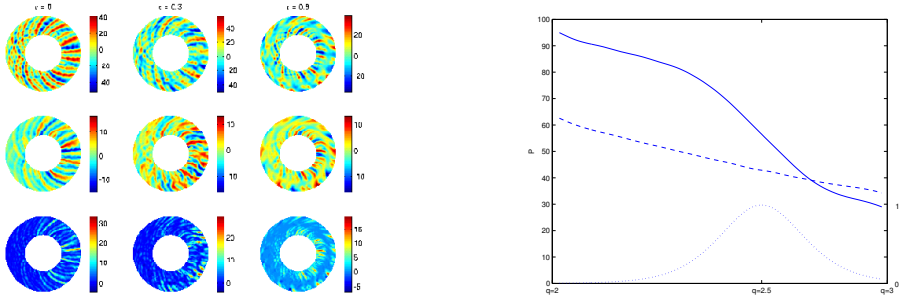

FIG. 1: (Left) Contour plots for electrostatic potential fluctuations, in the poloidal plane for three values of shear ($\epsilon = 0, 0.3, 0.9$). (Right) Equilibrium pressure profile for the shearless case (dashed line) and strong rotation shear (solid line). Dotted lines stands for the radial profile of the shear flow

The formation of the large turbulent eddies is clearly seen in these simulations (Fig.1 (Left), left column). The structures are modified in the presence of the $\mathbf{E} \times \mathbf{B}$ flow shear and fully destroyed when the rotation shear is large (Fig.1 (Left), right column).
The formation of a transport barrier in the region of large shear is clearly seen when $\epsilon = 0.9$ (Fig.1 (Right), solid curve) in contrast to the shearless case (Fig.1 (Right), dashed curve). This transport barrier on the pressure profile is a consequence of the reduction of the turbulent flux due to the imposed $E \times B$ shear. The turbulent flux is calculated as a product of the fluctuations of pressure and radial velocity and the cosine of their cross–phase[8] :

$$\Gamma = <\delta p\ \delta v_r> = <\delta p^2>^{1/2} <\delta v_r^2>^{1/2}\ \cos\ \delta_{v_r p} \qquad (3)$$

where the <> stands for the averaging over the fluctuation time and scale (in the poloidal and toroidal direction). Thus, the reduction of the turbulent flux may occur due to the reduction of the fluctuations amplitudes or/and the cross-phase between the pressure and potential fluctuations. Figure 2 (right) illustrate the effect of $E \times B$ shear on the amplitudes of pressure and radial velocity fluctuations and on their cross–phase. The effect of the $\mathbf{E} \times \mathbf{B}$ shear flow on the fluctuations and of the cross–phase is shown in Fig.2 (right). This figure displays the rms (root mean square) amplitudes of the fluctuations and the cross–phase (squares)as a function of the flow shear as well as their scaling. Stars stands for the rms pressure calculated from the simulations and circles stand for the rms of the radial velocity.

The modification of the RBM properties in the presence of the $E \times B$ rotation shear leads to the changes of the local transport. The effect of the $E \times B$ shear suppression of the anomalous transport is shown in Fig. 2 (left) where the local turbulent diffusivity ($\chi_{turb} = - < \Gamma_{turb} > / \nabla p$) is plotted as a function of the $E \times B$ shear flow. To illustrate the effect of the $E \times B$ shear at each radial location, it has been normalized to its value obtained without shear.

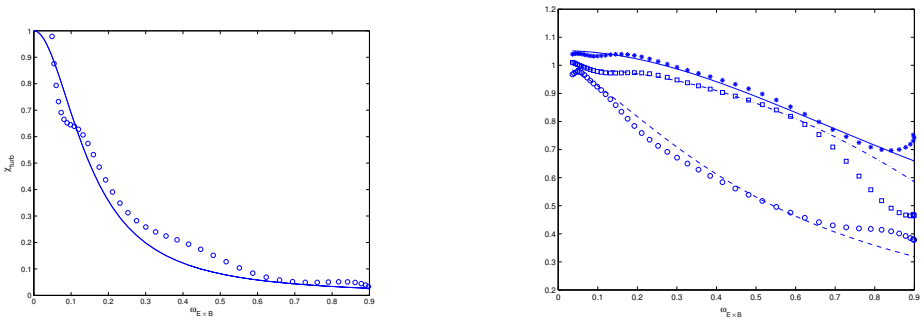

FIG. 2: (Left) Turbulent diffusivity as a function of the normalized $E \times B$ shear for two toroidal magnetic fields $B_0 = 1T$ (cross) $B_0 = 2T$ (circles). The solid line is a fit. (Right) Fluctuations level for RMS pressure (stars), radial velocity (circles), cross–phase (squares) respectively fitted with solid $f(\omega_{E\times B}) = 1/(1+0.7(\omega_{E\times B})^2)$, dashed $f(\omega_{E\times B}) = 1/(1+2.5(\omega_{E\times B})^{1.5})$ and dotted lines $f(\omega_{E\times B}) = 1-0.5(\omega_{E\times B})^2$.

The gradual reduction of the turbulent diffusivity with an increase of the $E \times B$ flow shear is obtained with full suppression of turbulent transport at a large shear ($\epsilon = 0.9$). The results shown in Fig. 2 (left) are used to deduce the rotation shear suppression scaling for the RBM–driven transport. The following dependence on the $E \times B$ rotation shear has been assumed for the turbulent diffusivity :

$$\frac{\chi_{turb}(\omega_{E\times B})}{\chi_{turb}(\omega_{E\times B}=0)} = \frac{1}{1+(\frac{\omega_{E\times B}}{\omega_c})^{\gamma}} \tag{4}$$

where the exponent γ and the correlation rate ω_c are supposed to be deduced from the simulations. The best fit of the numerical results shown in Fig.2 (Left) by the solid curves have been obtained assuming $\gamma = 2$ and $\omega_c^{-2} = \tau_c^2 = 45$ wich corresponds to a correlation time of the same order than found in our simulations . It should be mentioned the scaling for the RBM–driven transport with $\gamma = 2$ is similar to the scaling of an edge turbulence level with flow shear obtained analytically by Itoh and Itoh [19]. According to our simulations, the reduction of the turbulent transport mainly occurs at the moderate rotation shear while it is much weaker at large shear. Our χ–dependence is the one observed experimentally in edge biasing experiment on TEXTOR [17]. Also, the same scaling with the shear is studied for the fluctuations ($< \delta p^2 >^{1/2}, < \delta v_r^2 >^{1/2}$) and the cross–phase, where the results are summarized in Fig. 2 (Right). This figure displays RMS amplitudes of the fluctuations and the cross–phase as a function of the flow shear as well as their fit. Triangles stands for the simulated RMS pressure, the best fit (solid line) is obtained using the functional dependence of the form $f(\omega_{E\times B}) = 1/(1+(\tau_c * \omega_{E\times B})^2)$ following the model proposed by Shaing/Zhang–Mahajan [13, 14]. The same functional dependence (dashed line) is obtained for the RMS of the radial velocity (crosses). Concerning the cross–phase (squares), the best fit (dotted line) is obtained using the dependence $f(\omega_{E\times B}) = 1-(\tau_c * \omega_{E\times B})^2)$ only for a weak shear, that agrees with the Ware–Terry model[6], for a strong shear our results are consistent with the model of Terry et al. [20]. These numerical results are in good agreement with the experiments of Boedo et al.[10].

IV. SUMMARY AND DISCUSSION

The effect of imposed $E \times B$ rotation shear on the structure and properties of the RBM and associated turbulent transport has been studied using a 3D numerical code. It is shown that a large $E \times B$ shear modifies the radial structure of the modes being stretched poloidally. The reduction of the turbulent flux obtained in this case has been provided by the change of both amplitudes of the pressure and potential fluctuations and the relative phase between them.

The local turbulent transport has been analyzed and the $\mathbf{E} \times \mathbf{B}$ shear scaling of the turbulent diffusivity has been deduced from the fit of numerical results. We found that the power exponent ($\gamma = 2$) in the transport scaling in Eq. 4 is consistent with the $\mathbf{E} \times \mathbf{B}$ shear suppression of fluctuations as obtained in previous analytical model [13, 14], moreover concerning the scaling of the transport with the shear flow, the same $\gamma = 2$ dependance was found in the theoretical model of Itoh and Itoh [19]. The assumption of an imposed $\mathbf{E} \times \mathbf{B}$ shear makes our results relevant to the experiments with the edge biasing where the radial electric field providing the flow shear is externally controlled. The detailed experimental study of the $\mathbf{E} \times \mathbf{B}$ shear stabilization of the edge turbulence and transport has been performed for example in the TEXTOR tokamak[8, 16]. The comparison of these experimental results with our simulations show the following common features : Both in experiments and modelling the reduction in turbulence induced flux is mainly due to synergetic changes in the fluctuation amplitude and dephasing of the fluctuations [8]. The turbulence and turbulent transport are already affected at modest shear, i.e., partial stabilization of turbulence has been observed in experiments and reproduced in the simulations [8, 16]. The $\mathbf{E} \times \mathbf{B}$ shear scaling for a particle diffusivity obtained in experiments [17] is the same as one found for the turbulent diffusivity obtained in our simulations

---

[1] P. Beyer et al., Phys. Plasmas, **5**, 4271 (1998).
[2] B. A. Carreras et al., Phys. Fluids, **30**, 1388 (1987).
[3] T. S. Hahm et al., Phys. Fluids, **30**, 1452 (1987).
[4] T. S. Hahm et al., Phys. Fluids, **30**, 133 (1987).
[5] B. A. Carreras et al., Phys. Plasmas, **2**, 2744 (1995).
[6] A. S. Ware et al., Phys. Plasmas, **5**, 4271 (1998).
[7] P. Beyer et al., Plasma Phys. Contr. Fusion, **41**, A 757 (1999).
[8] J. A. Boedo et al., Nucl. Fusion, **40**, 1397 (2000).
[9] J. A. Boedo et al., Phys. Rev. Lett. **84**, 2630 (2000).
[10] J. A. Boedo et al, IAEA–CN–77/EXP5–22, (2000).
[11] H. Biglari et al., Phys. Fluids B, **2**, 1 (1990).
[12] R. E. Waltz et al., Phys. Plasmas, **1**, 2229, (1994).
[13] K. C. Shaing et al., Phys. Fluids B **2**, 1492 (1990).
[14] Y. Z. Zhang et al., Phys. Fluids B **4**, 1385 (1992).
[15] R. R. Weynants et al., Plasma Phys. Contr. Fusion, **35**, B177-B189 (1993).
[16] S. Jachmich et al., Plasma Phys. Contr. Fusion, **42**, A147-A152 (2000).
[17] S. Jachmich et al., Czech Journal of Phys., **49**, 191 (1999).
[18] R. J. Taylor et al. Phys. Rev. Lett. **63**, 2365 (1989).
[19] K. Itoh and S. I. Itoh, Plasma Phys. Contr. Fusion, **38**, 1 (1996).
[20] P. W. Terry, D. E. Newman and A. S. Ware, Phys. Rev. Lett., **87**, 185001–1 (2001).